Molecular Recognition and Reactivity of Ruthenium(II) Bipyridine Barbituric Acid Guests in the Presence of Complementary Hosts: Ruthenium(II) Promoted Enolization of Barbituric Acids in Guest−Host Complexes

Teen Chin, Zhinong Gao, Isabelle Lelouche, Yeung-gyo K. Shin, Ashok Purandare, Spencer Knapp,* and Stephan S. Isied*,†

Contribution from the Department of Chemistry, Rutgers, The State University of New Jersey, Piscataway, New Jersey 08855

Received May 7, 1997[⊗]

Abstract: The binding of the host **H1** (N,N′-bis(6-pivalamidopyrid-2-yl)-3,5-pyridinedicarboxamide) to three different ruthenium polypyridine complexes with an attached barbituric acid and barbital moieties (**RuG1**, **RuG2**, **RuG3**) (where **G1** = 5-[4-(4′-methyl)-2,2′-bipyridylidene]-2,4,6-(1*H*,3*H*,5*H*)-pyrimidinetrione**, G2** = 5-[4-(4′-methyl)-2,2′-bipyridyl]methyl-2,4,6-(1*H*,3*H*,5*H*)-pyrimidinetrione, and **G3** = 5-ethyl, 5-[4-(4′-methyl)-2,2′-bipyridyl]methyl-2,4,6-(1*H*,3*H*,5*H*)-pyrimidinetrione) and **Ru** = (4,4′-di-*tert*-butyl-bpy)$_2$Ru (bpy = 2,2′-bipyridine) has been studied in chlorinated solvents by NMR and fluorescence titrations. Significant binding was only observed between **H1** and the **RuG2** series, while steric hindrance significantly diminished binding between **H1** and **RuG1** or **RuG3**. The high binding constant for **RuG2** was related to the presence of the enolate form of the barbituric acid guest which forms strong H-bonds with the complementary host **H1**. For the organic barbituric acid and barbital guests, the keto and enol bind only weakly to **H1** ($K \sim 10^2$ M^{-1}); binding is further increased in the presence of base to generate the enolate. In contrast, formation of the **RuG2** enolate occurs upon binding to **H1** without any additional base. The ruthenium polypyridine cation (compared to the organic barbituric acid derivatives) facilitates ionization of the enol to enolate thus producing a better complementary H-bonding site between the guest and host. Molecular mechanics calculations confirmed the experimental observatons that the enolate has the highest binding constant to the Host **H1**, while the corresponding enol form has the weakest binding.

The design of synthetic guest and host molecules which undergo molecular recognition using weak noncovalent interactions is an emerging field[1] with many potential applications.[2−6] Multiple noncovalent interactions between guest and host molecules can result in strong binding even in highly polar solvents. These weak interactions can be major contributors to the binding of drugs to proteins and DNA targets and can form the basis for developing sensors to monitor the concentration of specific ions or molecules.[2−6]

Molecules with H-bonding recognition sites as their primary charge-transfer pathway are important for understanding the role of the electronic structure of peptides in controlling charge transport processes, especially those occurring in weakly polar protein interfacial environments.[7] Several model systems describing charge transfer processes that occur across H-bonding interfaces have been reported.[8−18]

We have demonstrated the presence of efficient long-range electron-transfer pathways in conformationally rigid peptides that are covalently linked to metal ion donors and acceptors.[19,20] In extending these studies to noncovalently linked donors and acceptors, we selected ruthenium(II) polypyridine barbituric

† E-mail address: Isied@rutchem.rutgers.edu.

⊗ Abstract published in *Advance ACS Abstracts,* December 15, 1997.

(1) For a recent general review in this area, see: Lawrence, D. S., Jiang, T., Levett, M. *Chem Rev.* **1995**, *95*, 2229.

(2) Feibuch, B.; Figueroa, A.; Charles, R.; Onan, K. D.; Feibush, P.; Karger, B. L. *J. Am. Chem. Soc.* **1986**, *108*, 3310.

(3) Carmack, G. D.; Freiser, H. *Anal. Chem.* **1977**, *49*, 1577.

(4) Steinbeck, M.; Ringsdorf, H. *J. Chem. Soc., Chem. Commun.* **1996**, 1193.

(5) Bethell, D.; Dougherty, G.; Cupertino, D. C. *J. Chem. Soc., Chem. Commun.* **1995**, 675.

(6) (a) Szemes, F.; Hesek, D.; Chen, A.; Dent, S. W.; Drew, M. G. B.; Goulden, A. J.; Graydon, A. R.; Grieve, A.; Mortimer, R. J.; Wear, T.; Weightman, J. S.; Beer, P. D. *Inorg. Chem.* **1996**, *35*, 5868. (b) Beer, P. D.; Chen, S.; Goulden, A. J.; Grieve, A.; Hesek, D.; Szemes, F.; Wear, T. J. *J. Chem. Soc. Chem. Commun.* **1994**, 1269. (c) Beer, P. D.; Drew, M. G. B.; Hazlewood, C.; Hesek, D.; Hodacova, J.; Stokes, S. E. *J. Chem. Soc., Chem. Commun.* **1993**, 229. (d) Beer, P. D.; Szemes, F. *J. Chem. Soc., Chem. Commun.* **1995**, 2245. (e) Beer, P. D.; Dent, S. W.; Wear, T. J. *J. Chem. Soc., Dalton Trans.* **1996**, 3241.

(7) For an interfacial electron transfer protein−protein structure, see: Pelletier, H.; Kraut, J. *Science* **1992**, *258*, 1748.

(8) Chang, S. K.; Hamilton, A. D. *J. Am. Chem. Soc.* **1988**, *110*, 1318.

(9) (a) Tecilla, P.; Dixon, R. P.; Slobodkin, G.; Alavi, D. S.; Waldeck, D. H.; Hamilton, A. D. *J. Am. Chem. Soc.* **1990**, 112, 9408. (b) Chang, S. K.; Engen, D. V.; Fan, E.; Hamilton, A. D. *J. Am. Chem. Soc.* **1991**, 113, 7640. (c) Hamilton, A. D. Advances in Supramolecular Chemistry, Gokel, G. W., Ed.; **1990**, 1, 1. JAI Press LTD. London, England.

(10) (a) Roberts, J. A.; Kirby, J. P.; Nocera, D. G.; *J. Am. Chem. Soc.* **1995**, *117*, 8051. (b) Turro, C.; Chang, C. K.; Leroi, G. E.; Cukier, R. I.; Nocera, D. G. *J. Am. Chem. Soc.* **1992**, *114*, 6233.

(11) (a) Bernan, A.; Izraeli, E. S.; Lavanon, H.; Wang, B.; Sessler, J. L. *J. Am. Chem. Soc.* **1995**, *117*, 8252. (b) Sessler, J. L.; Bing, W.; Harriman, A. *J. Am. Chem. Soc.* **1993**, *115*, 10418. (c) Harrriman, A.; Magda, D.; Sessler, J. L. *J. Am. Chem. Soc., Chem. Commun.* **1991**, 345. (d) Harriman, A.; Magda, D. J.; Sessler, J. L. *J. Phys. Chem.* **1991**, *95*, 1530. (e) Harriman, A.; Kubo, Y.; Sessler, J. L. *J. Am. Chem. Soc.* **1992**, *114*, 388.

(12) de Rege, P. J. F.; Williams, S. A.; Therien, M. J. *Science* **1995**, *269*, 1409.

(13) Yang, J.; Seneviratne, D.; Arbatin, G.; Andersson, A. M.; Curtis, J. C. *J. Am. Chem. Soc.* **1997**, in press.

(14) Aoyama, Y.; Asakawa, M.; Matsui, Y.; Ogoshi, H. *J. Am. Chem. Soc.* **1991**, *113*, 6233.

(15) Miyasaka, H.; Tabata, A.; Kamada, K.; Mataga, N.; *J. Am. Chem. Soc.* **1993**, *115*, 7335.

(16) (a) Zerkowski, J. A.; Seto, C. T.; Whitesides, G. M. *J. Am. Chem. Soc.* **1992**, *114*, 5473. (b) Seto, C. T.; Whitesides, G. M. *J. Am. Chem. Soc.* **1991**, *113*, 712.

(17) (a) Lehn, J. M.; Mascal, M.; DeClan, A.; Fischer, J. *J. Chem. Soc., Perkin Trans.* 2 **1992** 461. (b) Lehn, J. M.; DeClan, A.; Fischer, J. *J. Chem. Soc., Chem Commun.* **1990**, 479.

(18) Motesharei, K.; Myles, D. C. *J Am. Chem. Soc.* **1994**, *116*, 7413.

S0002-7863(97)01481-9 CCC: $14.00

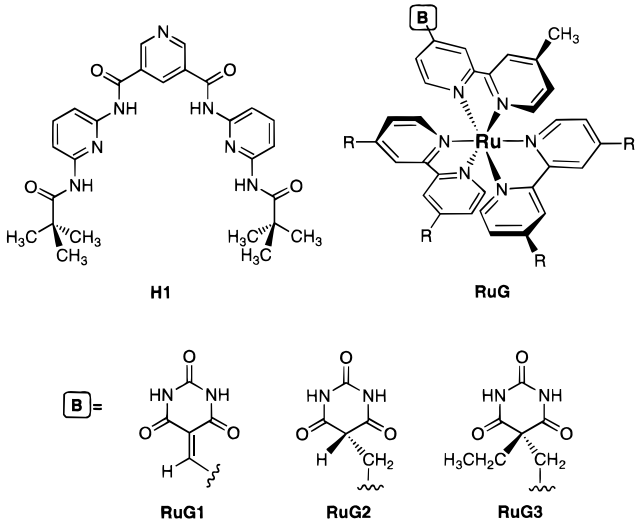

Figure 1. Molecular structure of the Host, **H1,** and three different ruthenium polypyridine guests. For **RuG1** and **RuG3**, R = 4,4′-di-*tert*-butyl-bpy (bpy = 2,2′-bipyridine), and for **RuG2**, R = 4,4′-di-*tert*-butyl-bpy, 4,4′-dimethyl-bpy, and bpy**.**

acid derivatives as guest molecules with H-bonding molecular recognition properties for specific complementary host molecules.[9a] Alkylated barbituric acid guests and 2,4,6-triaminopyrimidines and 2,6-diaminopyridine amide hosts have been used to probe molecular recognition by H-bonding interactions in several studies.[8,9]

This paper reports on the interaction between ruthenium(II) polypyridine barbituric acid derivatives with a complementary host (N,N′-bis(6-pivalamidopyrid-2-yl)-3,5-pyridinedicarboxamide) **H1** (Figure 1). Unexpectedly high binding is observed when a ruthenium(II) polypyridine barbituric acid cation (with appropriate molecular architecture) binds to **H1**, compared to the binding of the analogous barbituric acid derivatives without the ruthenium(II) polypyridine. These high binding-constants are discussed in terms of the keto−enol equilibria of the barbituric acid induced by the substitution of ruthenium(II) polypyridine at the C-5 carbon of the barbituric acid.

Results and Discussion

Synthesis and Characterization of Guest and Host Molecules. The guest molecules in our studies were either dialkylated, unsaturated, or saturated at the barbituric acid C-5 position (Figure 1), but only the saturated derivatives can undergo keto−enol equilibria (Figure 2). Comparative binding of the barbituric acids, and their analogous ruthenium derivatives, to **H1** can be best discussed in terms of this keto−enol equilibria.

The barbituric acid derivatives shown in Figure 1 were synthesized from the corresponding aldehydes and barbituric acid (Scheme 1), except for **G3**, which was synthesized using a modified literature procedure[21] (Scheme 2). The **G2**, **RuG2**, and **B-C$_3$H$_6$** were all obtained by reduction of their respective unsaturated precursors. The synthesis of the guests **G1**, **G2** and their respective ruthenium(II) complexes **RuG1**, **RuG2** is shown in Scheme 1. **G3** and corresponding ruthenium complex, **RuG3**, are shown in Scheme 2. For **RuG1** and **RuG3**, R = 4,4′-di-*tert*-butyl-bpy (bpy = 2,2′-bipyridine), and for **RuG2**, R = 4,4′-di-*tert*-butyl-bpy, 4,4′-dimethyl-bpy, and bpy.

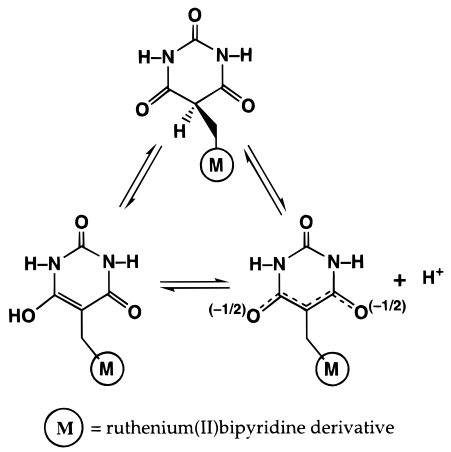

Figure 2. Keto, enol, and enolate forms of barbituric acid derivatives which are possible when C-5 has one or more protons attached to it.

The synthesis of **H1** is shown in Scheme 3. The pivaloyl group was used in order to increase the solubility and reduce aggregation[22] of the host molecules in low polarity solvents (such as CH_2Cl_2 and $CHCl_3$) where the binding of **H1** to barbituric acid derivatives was studied. The organic barbituric acid derivatives were characterized by NMR, HPLC, and mass spectrometric techniques, as described in the Experimental Section. In addition, UV−visible absorption, emission spectra, and oxidation/reduction potentials were measured for the ruthenium guest molecules. The complexes are all soluble in CH_2Cl_2 as their hexafluorophosphate salts, with **RuG2** being the most soluble. The absorption and emission spectra of the ruthenium polypyridyl barbituric acid derivatives (Table 1) bear close similarities to those of the parent compound $[Ru(bpy)_3]^{2+}$.[23] The oxidation and reduction potentials for the ruthenium complexes (in CH_3CN) are shown in Table 2.

Binding of Ruthenium Barbituric Acid Derivatives to H1 Host. The binding to **H1** of three closely related ruthenium bipyridine barbituric acid complexes (Figure 1), which differ in the mode of attachment of the barbital ring to the ruthenium bipyridine, was studied by NMR and fluorescence techniques. Only **RuG2**, the saturated analogue, can undergo keto−enol equilibria (enolization of the **RuG1** and **RuG3** barbituric acid complexes at C-5 is not possible). The binding of these ruthenium complexes to **H1** was carried out by following the change in the NMR chemical shift of amide protons of **H1** (and in some cases, the amide groups of the barbituric acid ring). Alternatively, changes in the fluorescence intensity of **RuG1**, **RuG2**, and **RuG3** were followed as **H1** was added.[24] Titration of **H1** with **RuG1** or **RuG3** did not show any measurable changes in the NMR of the amide protons of **H1** (in $CDCl_3$) or any measurable changes in the fluorescence signal intensity (in CH_2Cl_2). These results are consistent with immeasurably small binding between **H1** and **RuG1** and **RuG3**, respectively.

When **RuG2** was titrated with **H1** (in $CDCl_3$), large changes occur in the amide protons of **H1** and those of the barbituric acid ring of **RuG2** as shown in the NMR spectra in Figure 3.

(19) Isied, S. S.; Moreira, I.; Ogawa, M. Y.; Vassilian, A.; Arbo, B.; Sun, J. *J. Photochem. Photobiol. A: Chem.* **1994**, *82*, 203.
(20) Ogawa, M. Y.; Moreira, I.; Wishart, J. F.; Isied, S. S. *Chem. Phys.* **1993**, *176*, 589.
(21) Ciana, L. D.; Hamachi, I.; Meyer, T. J. *J. Org. Chem.* **1989**, *54*, 1731.
(22) Tamiaki, H.; Nomura, K.; Maruyama, K. *Bull. Chem. Soc. Jpn.* **1994**, *67*, 1863.
(23) Juris, A.; Balzani, V.; Barigelletti, F.; Campagna, S.; Belser, P.; von Zelewsky, A. *Coord. Chem. Rev.* **1988**, *84*, 85.
(24) Schneider, H. J.; Kraemer, R.; Simova, S.; Schneider, U. *J. Am. Chem. Soc.* **1988**, *110*, 6442.

Scheme 1. Synthesis of the Guests **G1** and **G2** and the Corresponding **RuG1** and **RuG2** Complexes

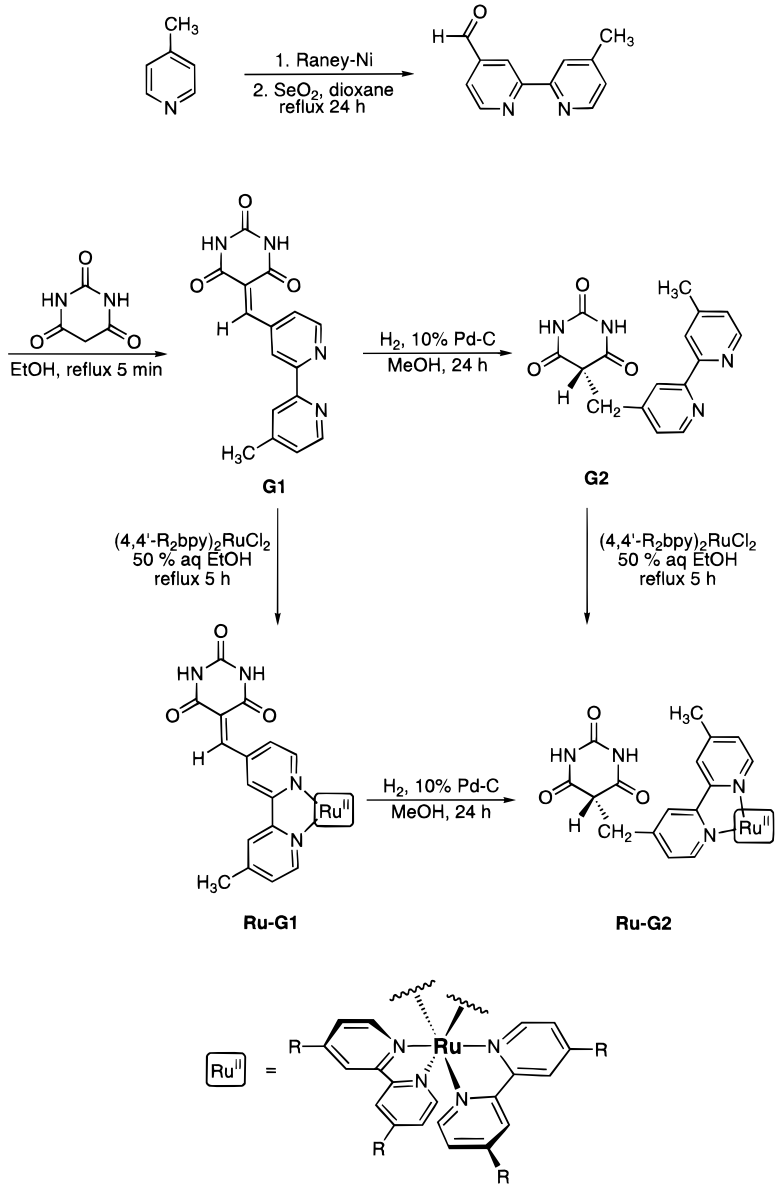

Scheme 2. Synthesis of the Guest **G3**

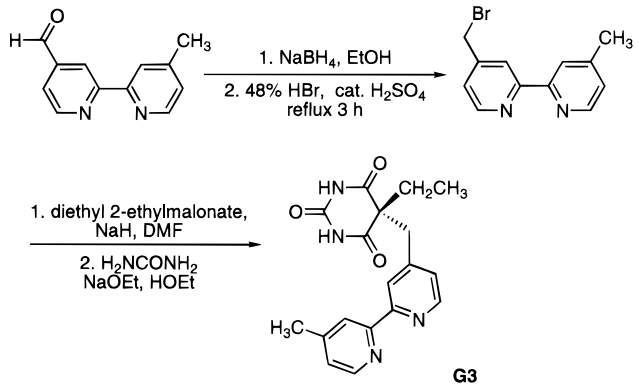

These changes are indicative of high binding constants. The NMR titration is used to obtain information on the stoichiometry (1:1) and binding of **H1** to **RuG2** and also to provide evidence on the molecular nature of the interaction between **H1** and **RuG2** (Figure 3). Additionally a Jobs plot of fluorescence changes also showed the 1:1 stoichiometry.[24] The binding constants for these 1:1 complexes were determined from the fluorescence changes that resulted when controlled amounts of **H1** were added to dilute solutions of **RuG2** ($\leq 5\ \mu$mol) (Figure 4).

To show that the binding is only sensitive to the barbituric acid substituted bipyridine derivative, three different complexes with substituents on the bipyridines not attached to the barbituric acid were synthesized and studied. These are (4,4′-di-*tert*-butyl-bpy)$_2$Ru**G2**, (4,4′-dimethyl-bpy)$_2$Ru**G2**, and (bpy)$_2$Ru**G2.** The solubility of these complexes in CH_2Cl_2 as PF_6 salts decreased as the size of the alkyl substituent decreased; however, the similar binding constants observed for these three **G2** derivatives with **H1** (Table 3) is strong evidence that they bind to **H1** in an almost identical manner.

The difference in binding of the respective ruthenium complexes to **H1** is related to the molecular architecture of the ruthenium barbituric acid complexes and to the cavity of the **H1** host. In **RuG1**, the olefinic carbon extends the planarity of the bipyridine ring, making the barbituric acid a poor fit for the cavity of **H1**. This poor fit, as shown by molecular modeling (vide supra), can explain the immeasurably low binding constant between **RuG1** and **H1**. For **RuG3**, higher binding to **H1** is predicted by molecular modeling methods; however, the binding is still not measurable experimentally. In **RuG3** (where a-

Scheme 3. Synthesis of the Host **H1** (R = Methyl and *tert*-Butyl)

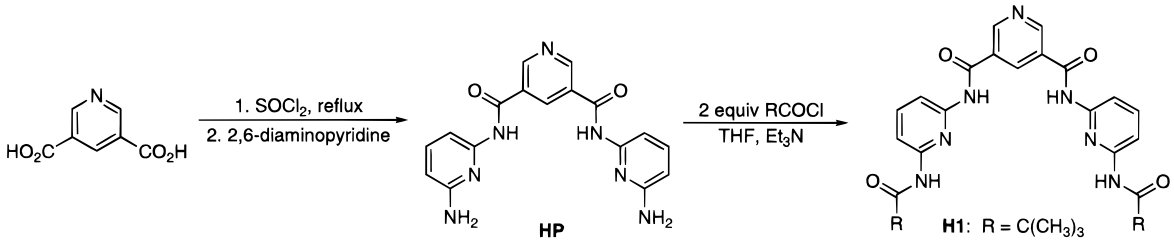

Table 1. Spectroscopic Data for the Ru(II) Polypyridyl Compounds in CH_2Cl_2 at 290 K

compounds	λ_{MLCT} (nm)	λ_{em}(nm)
$[(DTB\text{-}bpy)_2Ru(\mathbf{G1})]^{2+}$	462	610
$[(DTB\text{-}bpy)_2Ru(\mathbf{G2})]^{2+}$	462	610
$[(DTB\text{-}bpy)_2Ru(\mathbf{G3})]^{2+}$	462	610
$[(DTB\text{-}bpy)_3Ru]^{2+}$	460	607
$[(bpy)_2Ru(\mathbf{G2})]^{2+}$	460	610
$[(4,4'\text{-}(CH_3)_2bpy)_2Ru(\mathbf{G2})]^{2+}$	462	610
$[(bpy)_3Ru]^{2+}$	454	594

Table 2. Oxidation and Reduction Potentials[a] for the Ru(II) Polypyridyl Compounds

	oxidation[c]		reductions[c]	
compounds[b]	E^o (+2/+3) (V)	E^o(+2/+) (V)	$E^o(+/\phi)$ (V)	$E^o(\phi/-)$ (V)
$[(DTB\text{-}bpy)_2Ru(\mathbf{G1})]^{2+}$	+1.18	−1.48	−1.69	−2.05
$[(DTB\text{-}bpy)_2Ru(\mathbf{G2})]^{2+}$	+1.18	−1.49	−1.74	1.97
$[(DTB\text{-}bpy)_2Ru(\mathbf{G3})]^{2+}$	+1.14	−1.48	−1.67	−1.96
$[(DTB\text{-}bpy)_3Ru]^{2+}$	+1.11			
$[(bpy)_3Ru]^{2+}$	+1.28	−1.35	−1.55	

[a] Scan rate = 0.2 V/s. [b] As their PF_6 salts. [c] Potentials are measured vs SSCE in 0.1 M n-Bu_4NPF_6 in acetonitrile.

CH_2 group connects the bipyridine ring and the barbituric acid C-5 position), the dihedral angle between the barbituric acid ring and the bipyridine ring is nearly perpendicular and thus not planar (compared to **RuG1**). This lack of planarity is expected to improve the steric effect of the bipyridine ring on the **H1** cavity, resulting in a better fit and higher binding; however, the bulky pivaloyl groups on **H1** reduce the binding of **RuG3** to **H1**, and thus no measurable binding is observed for this guest/host pair. Replacing the pivaloyl group with a less sterically demanding butanoyl group makes this host more accomodating for the bulky ruthenium polypyridine moiety. The binding of **RuG3** to a host with the n-butanoyl (instead of the pivaloyl) group becomes measurable from chemical shifts of the amide bonds in an NMR titration ($K \sim 80\ M^{-1}$).[25]

The binding of **RuG2** and **RuG3** to **H1** is expected to be similar, since the absence of the ethyl group on the barbituric acid ring in **RuG2** is not expected to be significant. Instead, the keto−enol capability of **RuG2** (Figure 2) provides a major difference between **RuG2** and **RuG3**, which accounts for the additional four to five orders of magnitude increase in binding constant of **RuG2** to **H1** over **RuG3**. The enolate form of **RuG2** (with a negative charge delocalized over the two oxygen atoms of the barbituric ring) provides a strong hydrogen bonding network with six contacts between the outer amide protons of **H1** and the negatively charged oxygen atoms of the barbituric acid ring (Figure 5). The enol form of **RuG2** cannot have high binding to **H1**, because the conjugation at the C-5 of the barbituric acid is broken and the hydrogen bonding symmetry required to match the host is disrupted.

(25) Ghaddar, T.; Isied, S. Manuscript in preparation for publication.

In agreement with this model, replacement of the pivaloyl groups on **H1** with less sterically demanding alkanoyl groups should result in even higher binding constants for **RuG2** to these new hosts.

Binding of Organic Barbituric Acid Derivatives to H1. In comparison to the high binding constant of **RuG2** to **H1**, the binding of barbituric acids to **H1** was only modest under the same conditions (in $CHCl_3$ and CH_2Cl_2). Their binding constants were determined from the change in the position of the amide N−H resonances of **H1** upon binding to the different barbituric acids.[26] Four derivatives soluble in $CHCl_3$ and CH_2Cl_2 (Figure 6) were examined for the effect of keto−enol equilibria on their binding constants to **H1**. For the **BC_3H_6**, **BCF_3**, both keto- and enol-forms are accessible (as seen by changes of the NMR chemical shift of the amide protons of **H1** in Figure 7),[27−30] while for the alkylated (**B**arbital) and unsaturated **BC_3H_3** barbituric acids, only keto forms are accessible.

The amount of the keto- and enol-forms of the barbituric acids in different solvents can be determined from the assignment of the multiplet C−H resonance for the carbon connecting the barbital to the organic group. From this assignment, the **BC_3H_6** exists only in the keto-form in $CHCl_3$ and in acetone, while **BCF_3** exists in both the keto- and enol-forms (6.5:1) in $CHCl_3$ and only in the enol-form (Figure 7b) in the more polar solvent acetone. **B**arbital and **BC_3H_3** exist only in the keto form. The binding to **H1** of **B**arbital, **BC_3H_3**, and **BC_3H_6** are all very similar (Table 3), since they have similar structures and all exist in the keto-form in $CDCl_3$. For **BCF_3**, where the presence of the electron withdrawing group (CF_3) (compared to **BC_3H_6**) enhances the enol formation (6.5:1 enol/keto in $CDCl_3$), a lower binding constant to **H1** is observe. This is consistent with the enol form disrupting the symmetry of the H-bonding network to **H1**.

In order to generate the enolate form of one of the barbituric acids, **BCF_3** was studied, since it already exists predominantly in the enol form in $CDCl_3$ (in contrast to **BC_3H_6**). An NMR titration of a 1:1 complex of **H1** and **BCF_3** with 1 equiv of the base (1,8-bis(*N*,*N*-dimethylamine)naphthalene (Proton Sponge)) is shown in Figure 8. Large changes in the amide chemical shift observed upon addition of this base are an indication of a strong binding. Four different types of protons show additional shifts upon titration of **BCF_3:H1** with base. These are the four amide protons on **H1** (a,b), the two NH of the barbituric group (c) and the CH_2 protons of the carbon that connects the barbituric

(26) (a) Wilcox, C. S.; Cowart, M. D. *Tetrahedron Lett.* **1986**, *27*, 5563. (b) Wilcox, C. S. *Frontiers in Supramolecular Organic Chemistry & Photochemistry*; Scheider, H. J.; Durr, H., Eds.; VCH: Weinheim, Germany, 1990.

(27) Ascenso, J.; Candida, M.; Vaz, T. A.; Frausto da Silva, J. J. R. *Inorg. Nucl. Chem.* **1981**, *43*, 1255.

(28) Neville, G. A.; Avdovich, H. W.; By, A. W. *Can. J. Chem.* **1970**, *48*, 2274.

(29) Glasel, J. A. *Org. Magn. Reson.* **1969**, *1*, 481.

(30) Kelly-Rowley, A. M.; Lynch, V. M.; Anslyn, E. V. *J. Am. Chem. Soc.* **1995**, *117*, 3438.

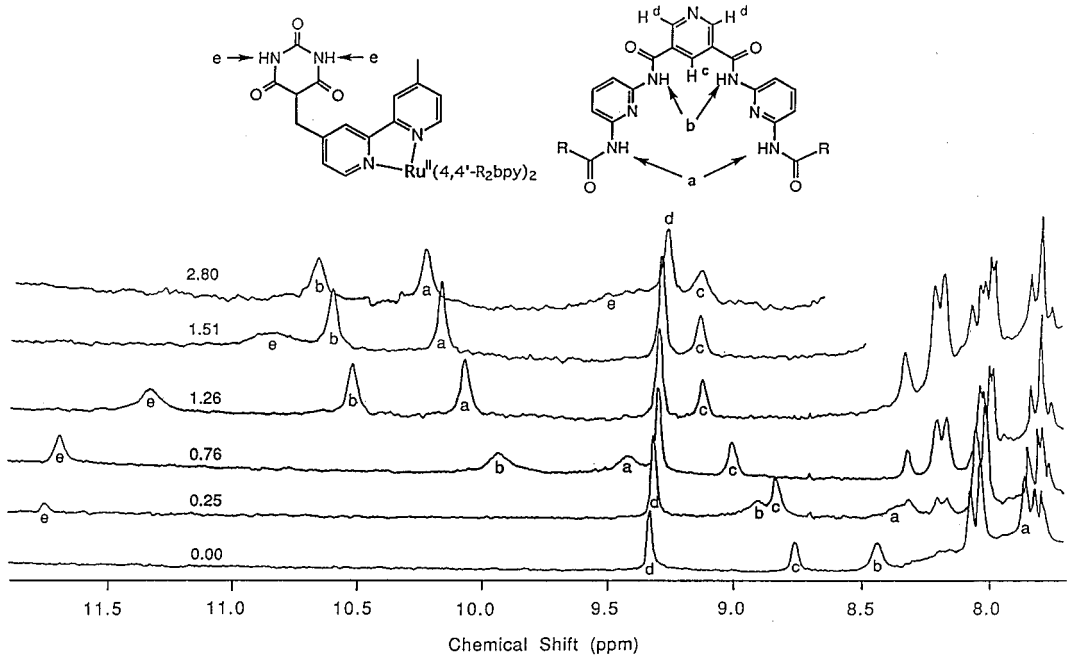

Figure 3. NMR Titration of **H1** (in $CHCl_3$) with varying amounts of **RuG2**. The guest and host are labeled and their assignment is labeled on the molecule and on the spectra as the binding between the guest and the host proceeds.

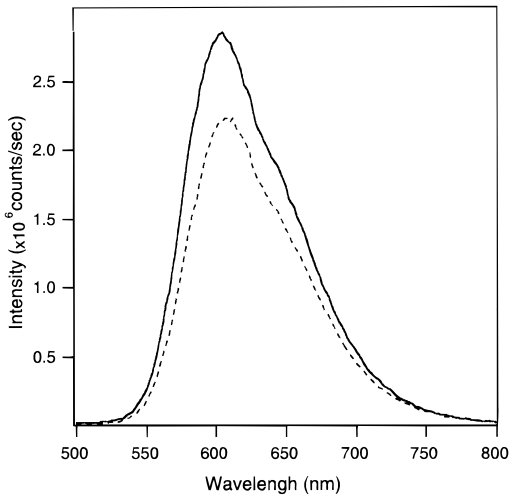

Figure 4. The fluorescence spectrum of **RuG2** (6.8×10^{-6} M in CH_2Cl_2) and the increase in intensity observed when excess **H1** (5.4×10^{-5} M) are added (λ_{exc}= 435 nm).

Table 3. Binding of Barbituric Acid Derivatives to Receptor **H1**

compounds	K_a (M^{-1})
$[(DTB\text{-}bpy)_2Ru(\mathbf{G1})]^{2+}$	<10 [a]
$[(DTB\text{-}bpy)_2Ru(\mathbf{G2})]^{2+}$	3.0×10^5 [a]
$[(DTB\text{-}bpy)_2Ru(\mathbf{G3})]^{2+}$	<10 [a]
$(4,4'\text{-}(CH_3)_2bpy)_2Ru(\mathbf{G2})]^{2+}$	2.8×10^5 [a]
$[(bpy)_2Ru(\mathbf{G2})]^{2+}$	3.1×10^5 [a]
Barbital	$4.5 \pm 1 \times 10^2$ [b]
$\mathbf{BC_3H_6}$	$4.7 \pm 1 \times 10^2$ [b]
$\mathbf{BC_3H_3}$	$5.3 \pm 1 \times 10^2$ [b]
$\mathbf{BCF_3}$	$0.7 \pm 0.3 \times 10^2$ [b]

[a] Obtained from fluorescence titration in CH_2Cl_2. [b] Obtained from ^{1}NMR titration data in $CDCl_3$.

acid ring to the organic substituent (d) (see also Figure 8). The strong binding is attributed to the formation of the enolate form of the $\mathbf{BCF_3}$ and an approximate binding constant, $K \sim 10^4$ M^{-1} can be calculated from the titration data.

The binding of the different forms of barbituric acids to the host **H1** is illustrated in Scheme 4. The strongest binding of barbituric acid derivatives to **H1** is observed when the barbituric

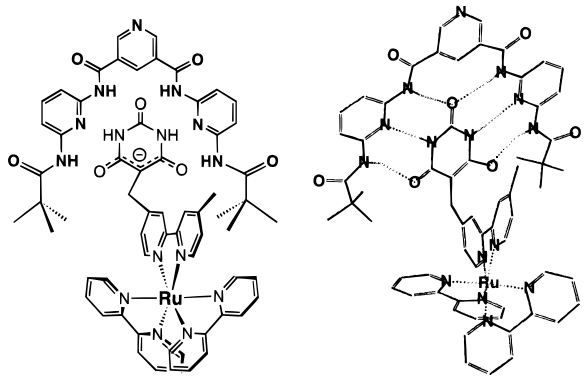

Figure 5. The molecular structure of the **RuG2:H1** complex (with the guest in the enolate form): formula (A) and the three-dimensional energy-minimized structure (B).

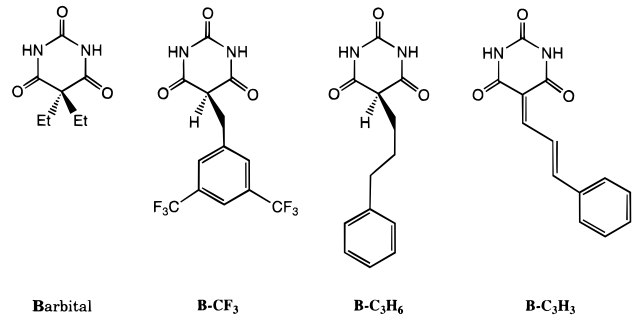

Figure 6. Barbital derivatives: alkylated, unsaturated, and reduced types.

acid is in the enolate form (which is a conjugated structure with a negative charge delocalized over three carbon and two oxygen atoms). Intermediate to weak binding is observed with barbituric acids that only exist in the keto form. The smallest binding occurs for the enol form because it disrupts the complimentary H-bonding of the guest to the host. In comparison to the **RuG2** complexes where strong binding to **H1** occurs, the barbituric acids without ruthenium studied show that both the presence of electron withdrawing groups on the barbituric acids

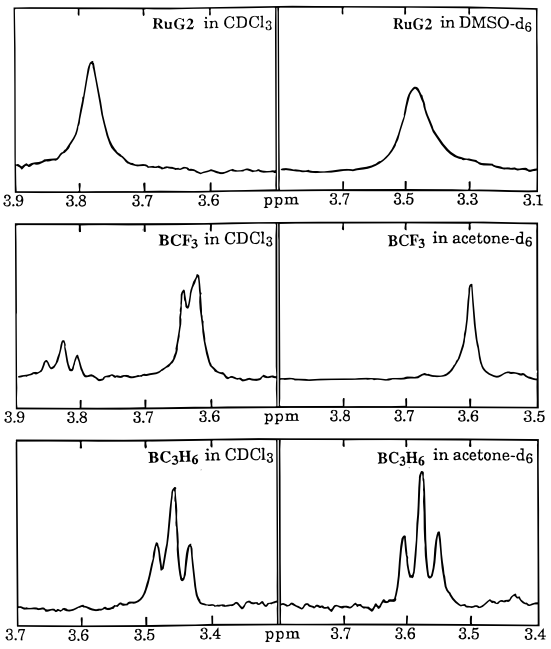

Figure 7. NMR of the C-5 protons in $\mathbf{BC_3H_6}$, $\mathbf{BCF_3}$, and **RuG2** in different deuterated solvents.

and the addition of a strong base are required to affect a similarly strong binding to **H1**.

Binding of Alkylated Barbitals to Related Receptors. The binding of barbital and alkylated barbitals to a number of linear and macrocyclic receptors was studied by Hamilton and coworkers.[9a] In their studies, hosts similar to **H1** were used with *n*-butanamide instead of pivalamide side chains (Figure 1). Higher binding constants were reported (ranging from 10^4–10^6 M^{-1}) for hosts with favorably maximized electronic effects and alkylated barbitals with no ability to form keto−enol equilibria.[9a]

Comparison of the binding data reported for **H1** with those reported earlier lead to the conclusion that the bulky pivaloyl groups (used in **H1** to prevent aggregation) as well as the ruthenium polypyridine moiety present additional steric effects for the H-bonding cavity of **H1** and decrease the binding of **H1** to **RuG3** as shown in Figure 9. Whereas the more open structure of the porphyrin barbital with the phenyl spacer can accomodate **H1** without these additional steric effects, significant differences were found when the open porphyrin molecules were compared to the sterically hindered **RuG3**. The proximity of the $Ru^{II}(bpy)_2$ to the **H1** cavity and its octahedral geometry are therefore responsible for these additional steric effects (compared to the planar porphyrin that is connected to the barbital derivative by a phenyl spacer at the C-5 carbon). If a spacer such as a phenyl group is added to the **RuG3,** similar binding to the porphyrin barbital and other alkylated barbitals would be expected. However, the extent to which such a spacer will reduce the capability of ruthenium polypyridine barbituic acid derivatives to undergo keto−enol equilibria is not known at this time.

The formation of the **RuG2** enolate causes C-5 to change from sp^3 to sp^2 and as a result moves the barbituric ring away from the bipyridine ligands (Figure 10) which increases the binding of **RuG2** to **H1** because of a modified H-bonding network. The sp^2 carbon formed upon enolization also strengthens H-bonding between the negatively charged oxygen atoms and the amide N−H's of the **H1** host. Future studies will be directed toward exploiting the keto−enol equilibria affected by the ruthenium complex as the steric effects induced by the pivaloyl groups are removed and other changes promoted by the 2,6-diaminopyridine rings are added.[25] Such molecular assemblies should result in increased binding constants and make detailed studies of electron transfer and energy transfer across H-bonding networks possible.

Using 2,6-dicarboxypyridine as part of the molecular design of **H1** is also useful for the attachment of kinetically inert metal ions such as Ru^{III}, Co^{III}, or Os^{III}, to the central pyridyl nitrogen in order to study intramolecular energy transfer and electron transfer across these hydrogen bonding networks.

Estimation of Binding Constants from Molecular Modeling Calculations. The binding of the guests to **H1**, K'_{eq}, was calculated by considering the enthalpy, $\Delta H°$, instead of the free energy, $\Delta G°$, for the association of **H1** with guests (and thus the prime notation in K'_{eq}). Although the $\Delta S°$ upon binding may not be negligible, the $\Delta S°$ of these reactions is expected to remain roughly the same for the series of reactions studied. Solvent effects for the different guests were also assumed to be constant throughout the series. With these approximations, the binding constants were calculated and used to predict the relative binding for different guest−host combinations.

The enthalpy change for the formation of the guest-host complex, guest + **H1** (host) → [guest-**H1**], is defined as $\Delta H° = H°$[guest-**H1**] $- H°$(guest) $- H°$(**H1**). The binding constants calculated from $K'_{eq} = e^{-\Delta H°/RT}$ at 25 °C (RT = 0.592 kcal) and the $H°$[guest-**H1**], $H°$(guest), and $H°$(**H1**) obtained from the energetics of the optimized structures for the guest−host molecules are described below.

The host molecule **H1** was assumed to have a planar structure (except for the pivaloyl group). The host **H1** structure can be optimized to either the *cis* or *trans*-conformation with respect to the C═O bonds closest to the central pyridine ring. Only the *cis*-conformation can form the experimentally derived 1:1 guest/host complex, while the *trans*-conformation can lead to a polymeric structure. The *cis*-conformation (minimized energy −112.0 kcal/mol) was used even though the *trans*-conformation has lower energy (minimized energy −118.1 kcal/mol) and is therefore more stable than the *cis*-conformation by ∼6 kcal/mol.

In the unsaturated **G1** and in **RuG1**, the dihedral angle of the barbiturate ring and the bipyridine moiety was found to be ∼60°, indicating steric interaction between the carbonyl group and the hydrogen at the 3-position of the bipyridine rings. A grossly distorted ring structure results when **RuG1** is introduced into the cavity of **H1**, because the pivaloyl group cannot fit well into the groove between the two bipyridine ligands of the $Ru^{II}(bpy)_2$. Thus, an extremely small binding constant is calculated for **RuG1** (Table 4). Experimentally the binding constant was not measurable ($K < 10$ M^{-1}).

For the **G2** and **RuG2**, the reduced olefinic minimized bridge structure takes a *cis* arrangement with respect to the barbiturate ring so that the bipyridine group is almost stacked on top of the barbiturate ring. Upon formation of the **G2** enol or enolate, the planes of the bipyridine and the barbiturate rings become perpendicular to each other and therefore relieve the steric constraints imposed on the **RuG1** conformation (i.e., interacting with the pivaloyl groups) (Figure 11). The enolate form of **G2** possesses a mirror plane with a bipyridine group that bisects the barbiturate ring when the orientation of peripheral bipyridine groups on the ruthenium are ignored. Therefore, the **RuG2** complex fits well into the **H1** cavity, resulting in high binding. In the enol form, the hydroxyl group breaks the symmetry, disrupts the H-bonding between the guest and the host and results in lower binding (Table 4). The **G3** only exists in the keto form, because of the replacement of hydrogen by the ethyl group at the carbon of the barbituric acid ring in **G3**.

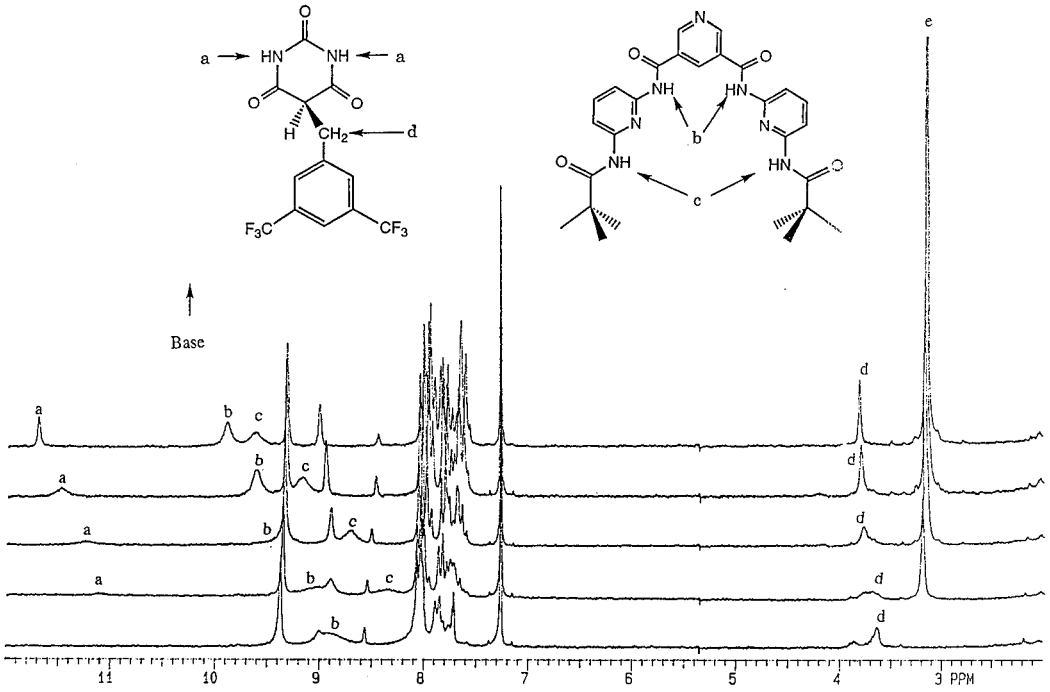

Figure 8. NMR titration of a 1:1 complex **BCF$_3$:H1** with the base, 1,8-bis-(*N*,*N*-dimethylamine)naphthalene (proton sponge). Shift in the amide protons upon binding is labeled on the molecule and on the spectra. e is the signal for the *N*,*N*-dimethyl of the proton sponge.

Scheme 4. A Scheme (Shown for the **BCF$_3$** Derivative) for the Binding of Organic Barbituric Acid Derivatives in Their Different Forms (Keto, Enol, Enolate) to the Host **H1** Showing That the Enolate Exhibits the Strongest Binding and the Enol Exhibits the Weakest Binding

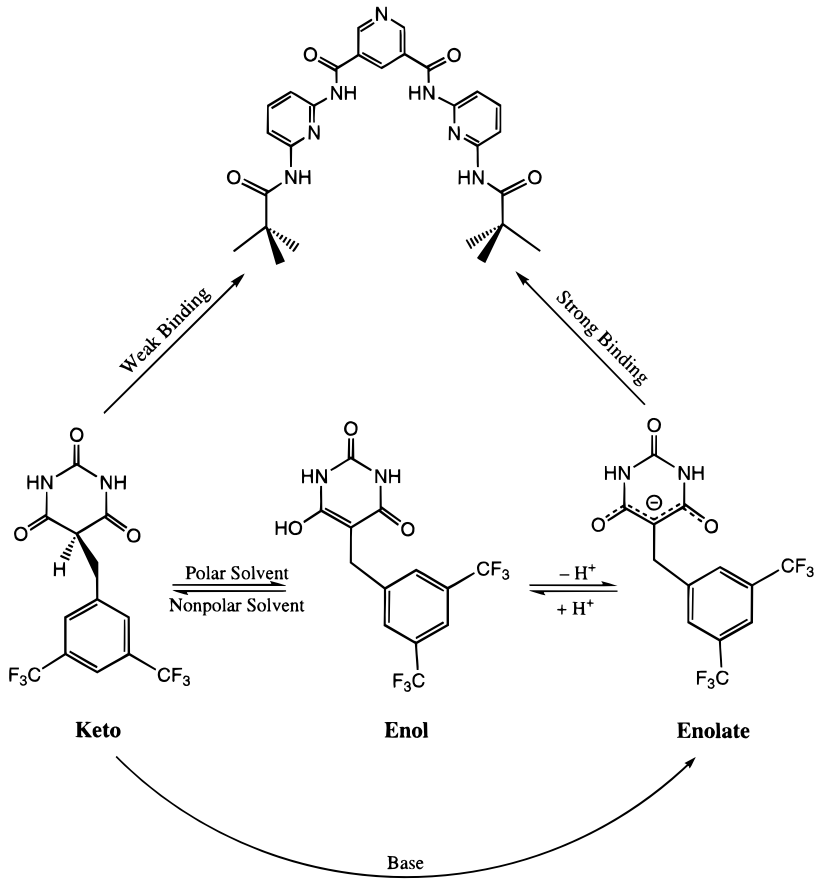

The interaction of **H1** with **RuG2** using the rigid geometry of **RuG3** is expected to improve its binding relative to **RuG2** to **H1** in its keto form (Table 4). The diethyl group of **G3** is assumed to have an all *trans*-conformation with the axis of the hydrocarbon chain perpendicular to the barbiturate ring. The binding constants based on the MM2 calculation (with the assumptions outlined in the beginning of this section) increase in the following order: K'_{eq}(enol) < K'_{eq}(keto) < K'_{eq}(enolate) (Table 4). Experimental observations agree with the trend predicted by these MM2 calculations.

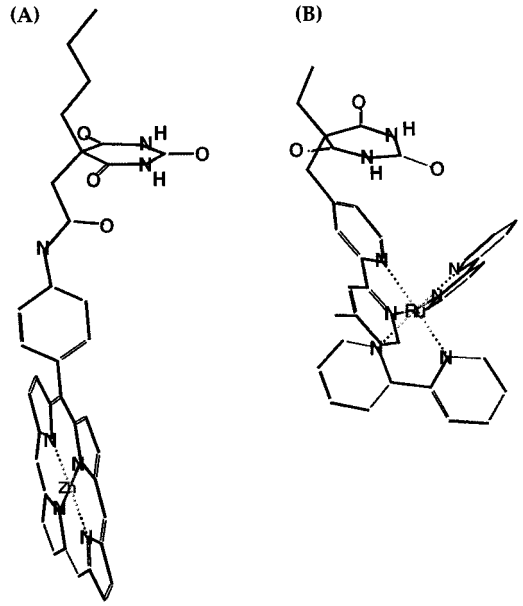

Figure 9. Comparison of the environment around the barbital group in the open porphyrin guest/host system (A) and in the sterically hindered ruthenium system (B).

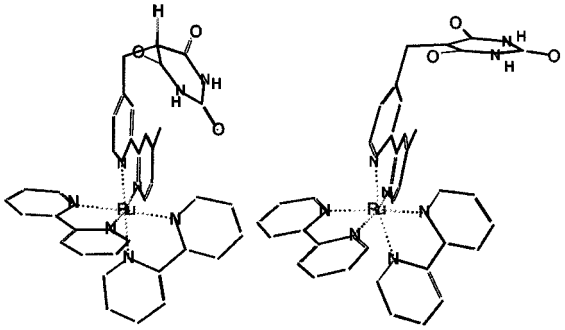

Figure 10. Three-dimensional structure of **RuG2** in the keto and in the enolate form showing the relief from steric interactions that enolate formation causes by changing C-5 from sp^3 to sp^2 carbon.

Table 4. Calculated Energetics of Host−Guest complexes with **H1** ($H = -112.0$ kcal/mol)

	energy, kcal/mol			
guest	*H*(guest)	*H*(guest−host)	ΔH	$e^{-\Delta H/RT}$
G1	−83.1	−210.3	−15.1	1.2×10^{11}
G2	−80.6	−211.7	−19.1	1.0×10^{14}
G3	−77.1	−209.4	−20.3	7.6×10^{14}
Barbital	−64.6	−194.6	−18.0	1.4×10^{13}
RuG1	−46.0	−114.7	43.3	1.8×10^{-32}
RuG2 (keto)	−42.9	−160.6	−5.6	1.4×10^{4}
RuG2 (enol)	−52.5	−164.5	0.0	1.0
RuG2 (enolate)	−54.4	−177.3	−10.8	7.8×10^{7}
RuG3	−46.1	−165.2	−7.0	1.3×10^{5}

Role of the Ruthenium Complex. The comparison of the binding constant for **RuG2** and **BCF_3** with **H1** shows that the ruthenium(II) complex favors the enolate formation more than the unchanged organic substituents. For the organic substituents with electron withdrawing substitutents (CF_3 groups) on the barbital ring (which enhance enol formation), enolate formation still requires the addition of a strong base. For the ruthenium derivatives no base is required to form the enolate. Upon the formation of the enolate, both the ruthenium barbituric acid and barbituric acids with organic derivatives strongly bind to **H1**.

The octahedral structure of the ruthenium complex also plays a role where the presence of the bipyridine rings close to **H1** can introduce large steric effects that reduce the binding between **H1** and the alkylated and unsaturated barbital derivatives through their interaction with the substituents at the two ends of the 2,6-diaminopyridine groups. Overall enhancement in binding of more than four orders of magnitude can result from enolate formation at the barbital ring. In this study the role of the pivaloyl substituents while useful in enhancing the solubility of the guest/host complex in weakly polar solvents and preventing aggregation, also turned out to sterically modulate the H-bonding association between the guest and the host. Other groups that can increase or decrease binding are currently under investigation.[25]

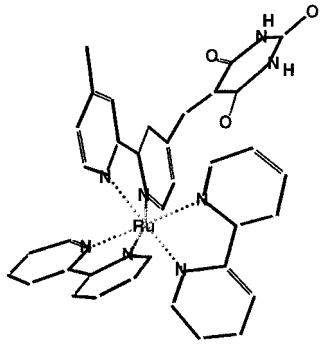

Figure 11. Three-dimensional structure of the **RuG1** complex showing the steric interaction between the barbituric acid ring and one of the bipyridine ligands attached to the Ru(II) complex.

Experimental Section

Solvents and Starting Materials. Chloroform was distilled from $CaCl_2$, CH_2Cl_2 and triethylamine from CaH_2, and THF from Na/benzophenone. For electrochemical experiments, commercial CH_3CN, dried over 4Å molecular sieves, was used without further purification. Commercial deuterated solvents were used as received. The 4,4′-di-*t*-Bu-2,2′-bipyridine[31] and cis-(4,4′-R-bpy)$_2$RuCl$_2$·2H$_2$O (where R = H, CH_3, *t*-Bu, and bpy = bipyridine) were prepared as described in the literature.[32a] The 4′-methyl-2,2′-bipyridine-4-carboxaldehyde[33] and 4-bromomethyl-4′-methyl-2,2′-bipyridine dihydrobromide were prepared by literature procedures.[21]

Instrumentation. HPLC was carried out by using a constant flow of the buffer (CH_3CN/H_2O/0.1% NaTFA) and monitoring at 254 nm. ^{1}H and ^{13}C NMR spectra were obtained at 200 MHz. Chemical shifts are reported in ppm downfield from tetramethylsilane, and coupling constants are in hertz. Fast atom bombardment mass spectra (FAB-MS) were taken at the Biomedical Research Core Facilities, University of Michigan; *m*/*z* values are reported for the protonated molecular ions unless otherwise indicated. Fluorescence spectra were obtained using a FluoroMax spectrofluorometer Model Spex 20. In voltammetric studies a three electrode cell configuration with a glassy carbon working electrode, a Pt auxiliary electrode, and a SCE reference electrode was used on a BAS 100A electrochemical analyzer. The reference electrode was placed in a glass tube separated from the bulk solution by a Vycor frit. After each determination, ferrocene was added to the sample solution, and its oxidation was measured voltammetrically for calibration. The supporting electrolyte in all cases was 0.1 M tetrabutylammonium hexafluorophosphate. The sample solutions, ~0.3−0.5 mM, were purged with argon for 15 min prior to the measurements. The reported $E_{1/2}$ values were obtained from the average of the cathodic and anodic peak potentials at varying scan rates. The redox couples were considered to have Nernstian behavior based on their peak-to-

(31) Sasse, W. H. F. *Org. Synth.* **1966**, *46*, 102.

(32) (a) Sullivan, B. P.; Salmon, D. J.; Meyer, T. J. *Inorg. Chem.* **1978**, *17*, 333. (b) Belser, V. P.; Zelewsky, V. A. *Helv. Chim. Acta* **1980**, *63*, 1675.

(33) (a) Peek, B. M.; Ross, G. T.; Edwards, S. W.; Meyer, G. J.; Meyer, T. J.; Erickson, B. W. *Int. J. Peptide Protein Res.* **1991**, *38*, 114. (b) Strouse, G. F.; Schoonover, J. R.; Duesing, R.; Boyde, S.; Jones, W. E., Jr.; Meyer, T. J. *Inorg. Chem.* **1995**, *34*, 473.

peak separations compared to that of the ferrocene/ferrocenium couple under the same conditions.

Binding Studies. The binding interaction between the receptor, **H1**, and various guest compounds was investigated by ^{1}H NMR and fluorescence spectroscopy.[26] The binding constants were obtained from a nonlinear least squares curve-fitting of the data to the binding isotherms. The protocol used for each technique is detailed below.

The fluorescence binding studies were all performed using CH_2Cl_2 (freshly distilled from CaH_2). The glass apparatus was predried in the oven just prior to use. To exclude moisture, the sample solutions were kept under an atmosphere of argon by using rubber septa and argon-filled balloons. In a typical binding experiment, a stock solution of the receptor **H1** (~0.5 mM) was added in aliquots of 5−10 μL to a solution of the ruthenium guest complex (~5 μM) of known concentration. The increase in emission intensity at 600 nm (for excitation at λ_{exc} = 435 nm) was monitored as a function of host concentration. Addition of **H1** was repeated until no further increase in emission intensity was observed.

The ^{1}H NMR binding studies were carried out in $CDCl_3$ or CD_2Cl_2 solution. In a typical experiment, the ^{1}H NMR spectrum of the solution of pure **H1** (2 mM in 0.5 mL of $CDCl_3$) was recorded first, and then small aliquots (5−50 μL) of the guest stock solution in $CDCl_3$ (25 mM, 0.2 mL) were added to the NMR tube via a gas tight syringe. The chemical shifts of the amide protons of the host were monitored as a function of guest concentration. Addition of guest was continued until no further shifts in the amide protons were observed.

Molecular Mechanics Calculations. All calculations were carried out using the Molecular Mechanics program (MM2),[36] a part of the CAChe WorkSystem (v. 3.8), from CAChe Scientific Co.

The initial structure of the host or guest moleculewas constructed assuming that the molecule is planar in the conjugated regions. Local minima were avoided by choosing the lowest energy configuration from a sequential minimization by varying all the dihedral angles of the inter-ring bonds in 12° steps. All the N−H and O═C bonds responsible for the hydrogen bonding in the host molecule were oriented toward the center so that the hydrogen bonding network would be intact. The selected structure was further optimized to within 0.0003 kcal/mol.

The $Ru^{II}(bpy)_2$ group was attached to the bipyridine side of the host molecules, and the coordination environment of this ruthenium was taken to be that of the crystal structure.[37]

Once the individual host or guest molecules were optimized, the oxygen atom of the pivotal O═C bond in the barbiturate ring was brought to 2Å distance from the para-H of the central pyridine of the host molecule with C═O···H angle of 180°. For the starting configuration, the 2, and 4-C's of the barbiturate ring of the guest molecules were placed in the same plane of the pyridine ring of the host, and the structure was then minimized to a limit of 0.0003 kcal/mol.

Preparation of Host Moleules. 3,5-Bis{[(6-amino-2-pyridyl)-amino]carbonyl}pyridine, HP. A slurry of 3.0 g (17.9 mmol) of 3,5-pyridine dicarboxylic acid in 2 mL of $CHCl_3$, 14 mL of thionyl chloride, and a drop of DMF was heated at reflux under an inert atmosphere for 5 h, resulting in a clear orange solution. The reaction mixture was concentrated under vacuum, and the resulting light orange solid was washed with benzene to remove remaining thionyl chloride. The solid was redissolved in 50 mL of CH_2Cl_2 and was added slowly via cannula to a vigorously stirred solution of 8.9 g (81.5 mmol) of 2,6-diaminopyridine in 6 mL of triethylamine and 200 mL of CH_2Cl_2 at 0 °C. The reaction mixture was allowed to warm to room temperature and then was stirred for 24 h. The reaction mixture was concentrated, and the resulting olive green solid was washed with water to remove excess 2,6-diaminopyridine and triethylamine hydrocloride. The crude product was purified by crystallization from tetrahydrofuran-heptane, affording 4.5 g (72%) of **H1** as a light greenish-yellow powder, mp > 200 °C (dec): ^{1}H NMR (DMSO-d_6) δ 5.83 (s, two N$\underline{H}_2$), 6.27 (d, J = 7.3, two pyr-H-3′), 7.40 (m, four pyr-H-4′,5′), 8.78 (s, pyr-H-4), 9.15 (d, two pyr-H-2,6), 10.43 (s, two CON$\underline{H}$); FAB-MS 350 $(M + H)^+$. Anal. Calcd for $C_{17}H_{15}N_7O_2 \cdot H_2O$: C, 55.58; H, 4.66; N, 26.69. Found: C, 55.48; H, 4.51; N, 25.90.

3,5-Bis{[6-(pivaloylamino)-2-pyridyl)amino]carbonyl}pyridine, H1. To a solution of 0.5 g (1.43 mmol) of **HP** and 0.89 mL (6.4 mmol) of triethylamine in 50 mL of anhydrous THF was added 0.35 mL (2.9 mmol) of pivaloyl chloride. After stirring at room temperature overnight, the reaction mixture was concentrated to a sticky yellow solid. Chromatography on silica gel using ethyl acetate/hexane (5:95) as the eluent yielded 250 mg (34%) of **H1**, mp 244−245 °C: ^{1}H NMR (DMSO-d_6) δ 1.25 (s, 18 C$\underline{H}_3$), 7.73 (m, two pyr-H-3′), 7.87 (m, four pyr-H-4′,5′), 8.82 (s, pyr-H-4), 9.26 (m, two pyr-H-4,6), 10.84 (s, four CON$\underline{H}$); FAB-MS 518 $(M + H)^+$.

Preparation of Organic Guest Molecules. 5-[4-(4′-Methyl)-2,2′-bipyridylidene]-2,4,6-(1*H*,3*H*,5*H*)-pyrimidinetrione, G1. 4-(4′-Methyl-2,2′-bipyridyl)carboxaldehyde (74.5 mg, 0.37 mmol) was added to a hot slurry of 55 mg (0.39 mmol) of barbituric acid in absolute ethanol, and the mixture was heated at reflux overnight. The light yellow precipitate was collected via filtration, washed with hot water (to remove unreacted barbituric acid), and then washed with absolute ethanol and finally ethyl ether. The product was dried under vacumn overnight to give 83.5 mg (73%) of **G1** as a bright yellow powder, mp > 200 °C: ^{1}H NMR (DMSO-d_6) δ 2.50 (s, bpy-4′-C$\underline{H}_3$), 6.14 (s, C═C$\underline{H}$−), 7.50 (d, J = 5.5, H-5′), 7.56 (d, J = 5.2, H-5), 8.15 (s, H-3′), 8.29 (s, H-3), 8.60 (d, J = 5.5, H-6′), 8.68 (d, J = 5.2, H-6), 10.23 (s, two N$\underline{H}$); FAB-MS 309 $(M + 1)^+$.

5-[4-(4′-Methyl)-2, 2′-bipyridyl]methyl-2, 4, 6- (1*H*,3*H*,5*H*)-pyrimidinetrione, G2. A slurry of 50 mg (0.16 mmol) of **G1** in 10 mL of DMF was saturated with H_2 for 30 min and then was treated with 10% Pd/C. After 12 h, the reaction mixture was filtered and then concentrated to give 32 mg (69%) of **G2**: ^{1}H NMR (DMSO-d_6) δ 2.40 (s, bpy-4′-C$\underline{H}_3$), 3.45 (s, C$\underline{H}_2$), 7.25 (d, J = 4.4, H-5,5′), 8.20 (s, H-3,3′), 8.51 (d, J = 4.4, H-6,6′), 11.11−11.25 (two N$\underline{H}$); FAB-MS 310 $(M + H)^+$.

5-Ethyl, 5-[4-(4′-Methyl)-2,2′-bipyridyl]methyl-2,4,6-(1*H*,3*H*,5*H*)-pyrimidinetrione, G3. Diethyl 2-ethylmalonate (0.18 g, 1 mmol) was added to a slurry of 30 mg (1.25 mmol) of NaH in 10 mL of dry DMF. Stirring was continued for about 30 min until a clear solution was obtained, and then 50 mg (2 mmol) of additional NaH was added. A solution of 0.42 g (1 mmol) of 4-bromomethyl-4′-methyl-2,2′-bipyridine dihydrobromide in 2 mL of DMF was added dropwise. The reaction was allowed to stir for 5 h. Water (2 mL) was added, and then the solution was neutralized with 10% aqueous HNO_3. The crude product, 4-(4′-methyl)-2,2′-bipyridyl)methyl malonate, was isolated by extraction with CH_2Cl_2 followed by concentration and then silica gel chromatography using CH_2Cl_2/EtOAc (8:2) as the eluant, resulting in 0.35 g (95%) of a light yellow oil. A solution of the crude product, 60 mg (1 mmol) of urea, and 0.6 mL of ethanolic sodium ethoxide (21% by weight) in 10 mL of absolute ethanol was heated at reflux for 2 h. Water (20 mL) was added, and the solution was acidified to pH 1 with 10% aqueous HNO_3. The resulting solution was cooled in the freezer overnight, and the product **G3** precipitated as a white crystalline solid, 0.2 g (67%), mp > 270 °C: ^{1}H NMR (DMSO-d_6) δ 0.79 (t, J = 7.3, $CH_2C\underline{H}_3$), 2.00 (q, J = 7.3, $C\underline{H}_2CH_3$), 2.39 (s, bpy-4′-C$\underline{H}_3$), 3.22 (s, C$\underline{H}_2$), 7.05 (d, J = 4.3, H-5′), 7.26 (d, J = 4.3, H-5), 8.10 (s, H-3′), 8.19 (s, H-3), 8.50 and 8.57 (two d, J = 4.3, H-6,6′), 11.52 (s, two N$\underline{H}$); FAB-MS 339 $(M + 1)^+$.

Barbituric Acid Derivatives. The 5-cinnamylidenepyrimidone-2,4,6-(1*H*,3*H*,5*H*)-trione[18] (**BC_3H_3**) described earlier was reduced to **BC_3H_6** with Pd/C (10%) as described for **G1** above. The 1-[3,5-ditrifluoromethylbenzene]methyl-2,4,6-(1*H*,3*H*,5*H*)-pyrimidinetrione (**BCF_3**) was prepared from 3,5-trifluoromethylbenzaldehyde and barbituric acid, followed by reduction with Pd/C (10%) using similar conditions to those used above for **G1** and **G2**. **B**arbital was synthesized as described previously.[34] All these organic derivatives were characterized by NMR in $CDCl_3$.

Preparation of Ruthenium Complexes: Ru(4,4′-di-*tert*-butyl-bpy)$_2$(G1)[PF$_6$]$_2$, RuG1. A slurry of 19.7 mg (0.064 mmol) of **G1** and 39.5 mg (0.531 mmol) of *cis*-Ru(4,4′-di-*tert*-butyl-bpy)$_2$Cl$_2$·2H$_2$O in 5 mL of ethanol/H_2O (70:30) was degassed with argon for 30 min and then heated at reflux under an argon atmosphere for 8 h, causing

(34) *A Textbook of Practical Organic Chemistry*; Vogel, A. I., Ed.; John Wiley and Sons: New York, 1956.

(35) Cowart, M.; Sucholeiki, I.; Bukownik, R. R. Wilcox, C. S. *J. Am. Chem. Soc.* **1988**, *110*, 6204.

(36) Allenger, N. L. *J. Am. Chem. Soc.* **1977**, *99*, 8127.

(37) Rillema, D. P.; Jones, D. S.; Levy, H. A. *J. Chem. Soc., Chem. Commun.* **1979**, 849.

the color to change from purple to bright orange. The solvent was removed by rotary evaporation, the resulting orange solid was redissolved in 2 mL of water, and then a saturated aqueous solution of NH_4PF_6 was added. The resulting orange precipitate was cooled in the freezer, filtered, and then washed with water and ethyl ether. The crude product was purified by adsorption chromatography on a neutral alumina column (2 × 15 cm) by using CH_3CN/H_2O (8:2) as the eluant, resulting in 50 mg (60%) of the complex, **RuG1**: ^{1}H NMR (DMSO-d_6): δ 1.36 (s, 36 C$\underline{H}_3$), 2.49 (s, bpy-4′-C$\underline{H}_3$), 6.02 (s, C═C$\underline{H}$), 7.20−7.59 (m, 12 bpy-H-3, 5), 8.25 (d, H-6′) 8.50 (s, H-6), 8.79 (s, 4 H-6″,6‴), 10.24 (s, two N$\underline{H}$); Neg-FAB-MS 1235 $(M - 1)^+$.

Ru(4,4′-di-*tert*-butyl-bpy)$_2$(G2)[PF$_6$]$_2$, RuG2. Complex **RuG2** was prepared by two different methods. In the first method, similar to that described for **RuG1**, a solution of 40 mg (0.054 mmol) of *cis*-Ru(4,4′-di-*tert*-butyl-bpy)$_2$Cl$_2$·2H$_2$O and 20 mg (0.064 mmol) of **G2** in 5 mL of 7:3 ethanol/H_2O was heated at reflux for 8 h under an argon atmosphere. After precipitation as its PF_6 salt by addition of a saturated solution of NH_4PF_6, the product was purified on a neutral alumina column by using CH_3CN/H_2O (95:5) as the eluant (24 mg, 60% yield). The second method involved the catalytic hydrogenation of **RuG1** in methanol. **RuG1[PF$_6$]$_2$** (56.7 mg, 0.056 mmol) was dissolved in 20 mL of methanol, and then the solution was saturated with H_2 for 1 h. Pd/C catalyst (10%, 30 mg) was added to the flask, and the reaction was allowed to proceed for 22 h. The **RuG2** was purified as described for **RuG1**, resulting in 70% yield (∼40 mg): ^{1}H NMR (DMSO-d_6): δ 1.37 (s, 36 (C$\underline{H}_3$), 2.49 (s, 3bpy-4′-C$\underline{H}_3$), 3.31 (s, CH_2), 7.20−7.59 (m, 12 bpy-H-3,5), 8.56 (s, H-6′), 8.62 (s, H-6), 8.81 (s, 4 H-4″, 6‴), 8.94 (s, 2 N$\underline{H}$); Neg-FAB-MS 1237 $(M - 1)^+$.

Ru(4,4′-di-*tert*-butyl-bpy)$_2$(G3)[PF$_6$]$_2$, RuG3. This complex was prepared in 60% yield as described above for **RuG1**: ^{1}H NMR ($CDCl_3$) δ 0.93 (t, J = 7.3, $CH_2C\underline{H}_3$), 1.39 (s, 36 CH_3), 2.19 (q, J = 7.3, C$\underline{H}_2$-CH_3), 2.55 (s, bpy-4′-C$\underline{H}_3$), 3.38 (s, CH_2), 7.20−7.60 (m, 12 bpy-H-3,5), 8.01 (s, H-6′), 8.10 (s, H-6), 8.15 (m, 4 H-6″,6‴), 8.68 (s, 2 N$\underline{H}$); Neg-FAB-MS 1265 $(M - 1)^+$.

Acknowledgment. This work was supported by the U.S. Department of Energy, Division of Chemical Sciences, Office of Basic Energy Sciences under contracts DE-FG05-90ER1410 and DE-FG02-93ER14356. We would also like to thank Professor C. Wilcox for sending us an early version of his program for the determination of binding constants by NMR.

JA971481Y